Solar Energy Materials & Solar Cells ∎ (∎∎∎∎) ∎∎∎–∎∎∎

Contents lists available at ScienceDirect

Solar Energy Materials & Solar Cells

journal homepage: www.elsevier.com/locate/solmat

Organic-silicon heterojunction solar cells on *n*-type silicon wafers: The BackPEDOT concept

Dimitri Zielke [a,*], Alexandra Pazidis [a], Florian Werner [a], Jan Schmidt [a,b]

[a] Institute for Solar Energy Research Hamelin (ISFH), Am Ohrberg 1, 31860 Emmerthal, Germany
[b] Institute of Solid-State Physics, Leibniz Universität Hannover, Appelstrasse 2, 30167 Hannover, Germany

ARTICLE INFO

Keywords:
Saturation current density
Solar cell
Heterojunction
Organic-silicon
PEDOT:PSS

ABSTRACT

We measure saturation current densities down to $J_0 = 80$ fA/cm^2 for organic-silicon heterojunctions with poly(3,4-ethylenedioxythiophene):poly(styrenesulfonate) (PEDOT:PSS) as an organic layer. This remarkably low J_0 value corresponds to implied open-circuit voltages around 690 mV, demonstrating the high-efficiency potential of this novel junction type. However, experimentally realized organic-silicon heterojunction solar cells showed relatively moderate efficiencies so far, typically below 12%. We demonstrate in this study that these solar cells were limited by the fact that the organic-silicon junction was localized on the cell front, resulting in a significant parasitic light absorption within the PEDOT:PSS layer. In addition, the rear surface of these front-junction solar cells was either poorly passivated or not passivated at all. In this paper, we overcome these limitations by proposing a back-junction organic-silicon solar cell, the so-called "BackPEDOT" cell. We show that placing PEDOT:PSS on the rear side instead of the front surface avoids parasitic light absorption within the PEDOT:PSS and allows for an improved surface passivation. We fabricate and characterize BackPEDOT solar cells and achieve very high open-circuit voltages of up to 663 mV and short-circuit current densities of up to 39.7 mA/cm^2. Despite the relatively high series resistances of our first BackPEDOT cells, we achieve an energy conversion efficiency of 17.4%. The measured pseudo efficiency of the best cell of 21.2% suggests that our novel BackPEDOT cell concept is indeed suitable for easy-to-fabricate high-efficiency solar cells after some further optimization to reduce the contact resistance between the PEDOT and the *n*-type silicon wafer. Based on realistic assumptions we conclude that Back PEDOT cells have an efficiency potential exceeding 22%.

1. Introduction

n-type crystalline silicon solar cells require a hole-conducting layer to form the electron–hole separating junction. State-of-the-art junctions are realized by technologically advanced methods, such as high-temperature boron diffusion [1] or the plasma deposition of boron-doped amorphous silicon (a-Si:H) [2]. Furthermore, a-Si:H causes parasitic light absorption, which can be reduced by implementing the junction on the rear surface of the solar cell [3,4]. A technologically much less demanding approach is the deposition of an organic *p*-type layer, such as poly(3,4-ethylenedioxythiophene): poly(styrenesulfonate) (PEDOT:PSS), on the *n*-type crystalline silicon base [5–8]. PEDOT:PSS is a transparent hole-conducting polymer with adjustable electrical parameters. Conductivities of up to 1000 S/cm and work functions in the range between 4.8 and 5.2 eV can be realized with this organic material. PEDOT:PSS can be easily deposited by spin, spray, dip coating and any other methods which are suitable for the deposition of an aqueous solution at temperatures as low as 100 °C [9] under atmospheric pressure conditions. On *n*-type silicon, PEDOT:PSS forms an organic-silicon junction with a remarkably low saturation current density of 80 fA/cm^2, as we have demonstrated in a recent publication [10]. However, the highest reported energy conversion efficiency of an organic-silicon solar cell up to now is only 12.3% [10]. Organic-silicon solar cells fabricated so far were all limited by the fact that the organic-silicon junction was localized on the front side of the solar cell, which results in a significant parasitic light absorption within the PEDOT:PSS layer. In addition, the rear surface of these front-junction solar cells was either poorly passivated or not passivated at all. In this work, we overcome these limitations by proposing a back-junction organic-silicon solar cell, the so-called "BackPEDOT" cell. We compare the short-circuit current density and the open-circuit voltage potential for front-junction and back-junction organic-silicon solar cell structures by means of ray tracing simulations and saturation current density measurements. Finally, we experimentally compare a front-junction organic-silicon solar cell with a BackPEDOT solar cell.

* Corresponding author. Tel.: +49 5151 999 635; fax: +49 5151 999 400.
E-mail address: d.zielke@isfh.de (D. Zielke).

http://dx.doi.org/10.1016/j.solmat.2014.05.022
0927-0248/

2. The BackPEDOT cell concept

Fig. 1 shows schematic drawings of (a) a front-junction organic-silicon heterojunction cell and (b) a back-junction ("BackPEDOT") solar cell. Both types of solar cells were made on *n*-type crystalline silicon with random-pyramid (RP)-textured front. An electron-conducting phosphorus-diffused n^+ region was either positioned on the front (Fig. 1(b), 'Front Surface Field', FSF) or on the rear (Fig. 1(a), 'Back Surface Field', BSF) to form an ohmic contact between the base and the metal contact. In-between the silicon wafer and the PEDOT:PSS layer we introduced an ultrathin passivation layer, which allows an effective hole transport (e.g., by means of quantum-mechanical tunneling) through it, in order to minimize interface recombination. In this study, we used a silicon oxide (SiO_x) layer grown in air at room temperature ('natural oxide'). The PEDOT:PSS layer was deposited either on the front surface creating a front-junction or on the rear surface creating a back-junction solar cell. The BSF of the front-junction solar cell was fully metalized by evaporated aluminum. The FSF of the BackPEDOT solar cell was passivated by SiN_x. In addition, an ultrathin AlO_x tunneling layer improves passivation between metal and silicon. Front metallization of the front-junction solar cell was realized by Titanium/Palladium/Silver (Ti/Pd/Ag) evaporation, whereas the rear surface of the back-junction solar cell was metalized with silver.

3. Saturation current density measurements

3.1. Organic-silicon heterojunction

Fig. 2(a) shows the lifetime test structure used to extract the saturation current densities J_0 of the organic-silicon junctions on random pyramid (RP)-textured and planar surfaces, respectively. The hole-conducting PEDOT:PSS layer was deposited on one side of the c-Si wafer and the other surface of the sample was passivated by silicon nitride (SiN_x), which was deposited by means of plasma-enhanced chemical vapor deposition (PECVD, Oxford Instruments, Plasmalab 80+) [11]. We used virtually undoped (~150 Ω cm) single-crystalline (100)-oriented 300 μm thick *p*-type float-zone (FZ) silicon wafers. After RCA cleaning of the silicon wafers, we deposited a 110 nm thick SiN_x surface-passivating layer on one side of the single-crystalline silicon (c-Si) wafer. Some c-Si wafers were then RP-textured on the bare wafer side in an anisotropic KOH/iso-propanol etching solution. In order to form a passivating tunneling layer between the organic layer and the c-Si wafer, a native oxide (SiO_x) was then grown by storing the wafer for 24 h in ambient air. Subsequently, the samples were coated with the PEDOT:PSS precursor (F HC Solar, Clevios Heraeus GmbH) by a spin-on technique (KarlSuss, SUSS SM 240) and dried on a hotplate at 130 °C for 30 s.

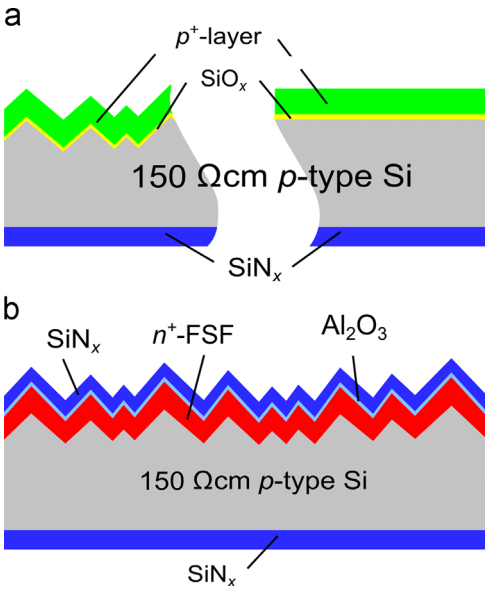

Fig. 2. Schematics of a lifetime test sample used to extract the saturation current density J_0 (a) of the silicon-PEDOT:PSS junction and (b) of the n^+ FSF region.

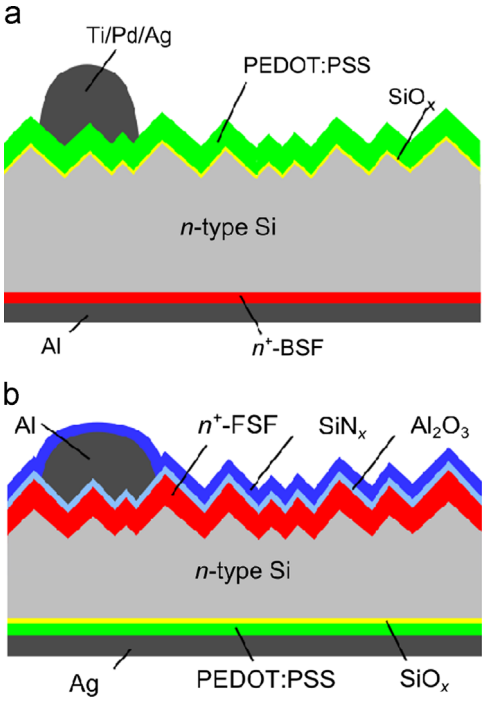

Fig. 1. Schematics of (a) a front-junction organic-silicon heterojunction cell and (b) a back-junction ("BackPEDOT") solar cell on *n*-type silicon.

3.2. Phosphorus-diffused homojunction

Fig. 2(b) shows the test structure used to determine the J_0 value of the FSF region. The SiN_x-passivated n^+ region was prepared on one side of the c-Si wafer and the other surface of the sample was only passivated by a SiN_x passivating layer. We used the same virtually undoped wafer material as in Section 3.1. After RCA cleaning of the silicon wafers, we deposited a 100 nm thick SiN_x surface-protecting layer on the rear side of the wafer. Afterwards, the wafers were RP-textured on the front side in an anisotropic KOH/iso-propanol etching solution. Subsequently, the samples were RCA-cleaned and a phosphorus diffusion was performed from a $POCl_3$ source in a quartz-tube furnace at 850 °C forming a FSF with a sheet resistance of 114 ± 11 Ω/sq. After removing the protecting SiN_x layer and the phosphorus silicate glass in dilute hydrofluoric acid, we deposited a 110 nm thick SiN_x surface-passivating layer at 400 °C on the entire rear surface. Afterwards, an 0.24 nm thick AlO_x tunneling layer was atomic-layer-deposited (FlexAL, Oxford Instruments) on the sample front surface [12] and the front surface was covered by a 10 nm surface-passivating SiN_x layer with a refractive index of 2.4 and an additional 70 nm SiN_x antireflection layer with a refractive index of 1.9 at a temperature of 330 °C.

Furthermore, we fabricated non-diffused reference samples passivated with SiN_x with a refractive index of 2.4 on both surfaces, where we measured an effective surface recombination velocity S_{SiN} in the range between 4 and 14 cm/s (at an excess carrier density in the range between 10^{14} and 10^{16} cm^{-3}) for the

Please cite this article as: D. Zielke, et al., Organic-silicon heterojunction solar cells on *n*-type silicon wafers: The BackPEDOT concept, Solar Energy Materials and Solar Cells (2014), http://dx.doi.org/10.1016/j.solmat.2014.05.022

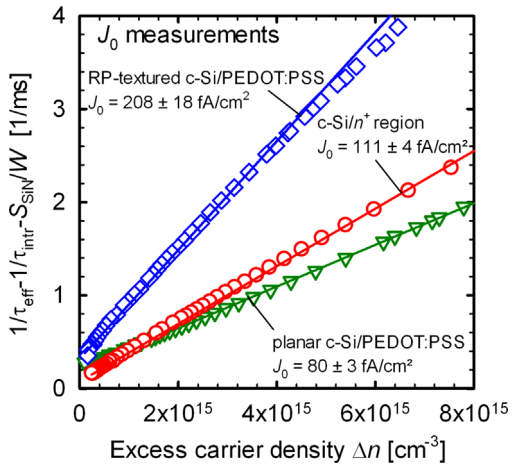

Fig. 3. Inverse effective lifetime $1/\tau_{eff}$ minus the inverse intrinsic lifetime $1/\tau_{intr}$ minus the surface-related lifetime S_{SiN}/W as a function of the excess carrier concentration Δn of a planar organic-silicon junction (green triangles), RP-textured organic-silicon junction (blue diamond) and RP-textured n^+ region (red circles). (For interpretation of the references to color in this figure legend, the reader is referred to the web version of this article.)

SiN_x-passivated surfaces. Saturation current densities J_0 were deduced from transient photoconductance decay (PCD) measurements using a WCT-120 lifetime tester from Sinton Instruments [13].

3.3. Experimental J_0 results

Fig. 3 shows the inverse effective lifetime $1/\tau_{eff}$ minus the inverse intrinsic lifetime $1/\tau_{intr}$ minus the surface-related lifetime S_{SiN}/W as a function of the excess carrier concentration Δn of a planar and a textured silicon-PEDOT:PSS sample, respectively. We extract a saturation current density $J_{0\_PEDOT\_planar}$ of only 80 ± 3 fA/cm^2 for the planar sample. Independent of the cell architecture, the measured J_0 of 80 fA/cm^2 corresponds to a V_{oc} potential of 692 mV for a realistic J_{sc} value of 40 mA/cm^2. This remarkably high V_{oc} value highlights the general high-efficiency potential of organic-silicon heterojunction solar cells.

Random-pyramid texturing of the silicon surface increases $J_{0\_PEDOT\_RP}$ to a value of 208 ± 18 fA/cm^2. We explain the increased J_0 value for textured samples by the increased surface area and the fact that PEDOT:PSS does not completely cover the textured surface. The RP-textured, phosphorus-diffused and SiN_x-passivated n^+ region exhibits J_{0_n+} of 111 ± 4 fA/cm^2. The metalized n^+ region exhibits $J_{0\_n+\_met}$ of 1250 fA/cm^2 [14].

4. Realistic prediction of the reachable open-circuit voltage

Based on our J_0 measurements presented in the previous Section, we can now calculate the realistic reachable V_{oc} of our organic-silicon solar cells using the following equation:

$$V_{OC} = V_T \ln\left(\frac{J_{sc}}{J_{0e}} + 1\right), \quad (1)$$

where $V_T = 25.7$ mV is the thermal voltage at a temperature of 25 °C and J_{sc} equals 34.7 mA/cm^2 and 41.1 mA/cm^2 for the front-junction and back-junction solar cell, respectively. These J_{sc} values are calculated from light absorption as we will show in the following Section 5. In the following, we calculate the maximal reachable V_{oc} of our front-junction and back-junction solar cells, respectively. Note that V_{oc} of our front-junction solar cell is largely limited by the fully metalized n^+ rear side exhibiting $J_{0\_n+\_met}$ of 1250 fA/cm^2 and V_{oc} of our back-junction solar is limited by the SiN_x passivated n^+ front exhibiting J_{0_n+} of 111 ± 4 fA/cm^2.

The total J_0 of the front-junction organic-silicon solar cell is calculated by adding the two contributions of the RP-textured silicon-PEDOT:PSS front and the fully metalized n^+ rear as follows:

$$J_{0\_front} = J_{0\_PEDOT\_RP} + J_{0\_n+\_met} = 1460 \text{fA/cm}^2. \quad (2)$$

The J_0 of the our BackPEDOT solar cell is calculated by adding the two contributions of the planar silicon-PEDOT:PSS rear surface and the SiN_x-passivated n^+ front as follows:

$$J_{0\_back} = J_{0\_n+} \times (1-M) + J_{0\_n+\_met} \times M + J_{0\_PEDOT\_plane} = 214 \text{fA/cm}^2, \quad (3)$$

where $M = 2$ % is the metallization fraction of our front grid. Since high-quality n-type silicon is used in our experimental cells, we neglect recombination within the base. Using Eqs. (2) and (3) we calculate open-circuit voltages V_{oc} of 614 mV and 668 mV for our front- and back-junction solar cells, respectively.

5. Realistic prediction of the reachable short-circuit current density

We calculate the realistically achievable J_{sc} values of our organic-silicon solar cells by simulating the light absorption using the ray tracing simulation tool Sunrays 1.3 [15]. The silicon bulk has a thickness of 160 μm for the back-junction and 300 μm for the front-junction solar cell. The pyramidal geometry is deduced from scanning electron microscopy images. In our model the base of a pyramid is 1.7 μm and the height of a pyramid is 1.2 μm. Order and thickness of dielectric layers are given in the solar cell experimental details in Section 6.1. Refraction index $n(\lambda)$ and extinction coefficient $k(\lambda)$ of silicon and the dielectric layers have been measured on reference samples. We determine the optical constants of a 100 nm PEDOT:PSS layer using spectral ellipsometry (M-2000, J.A. Woollam Co., Inc.) and transmission measurements (Cary 5000, Varian Inc.). To determine the optical constants, ellipsometric measurements of on silicon were performed. In addition the reflection and transmission of three layers with different thicknesses on float-glass were measured and fitted simultaneously with the ellipsometric data in the WVASE-software (J.A. Woollam Co., Inc., v. 3.774). The model consisted of a dominant Gaussian oscillator in the UV-region outside the measurement data range and a Lorentz oscillator in the IR-region. Four additional very broad Gaussian oscillators were used in the visible and NIR to account for the measured absorption. Further optional parameters are a poles in the far UV and far IR and an offset to the dielectric function. Fig. 4(a) shows measured $n(\lambda)$ and $k(\lambda)$ curves of our PEDOT:PSS material and for comparison that of a SiN_x antireflection coating.

We neglect any recombination losses, absorption within the "dead-layer" and shading by the front metallization to estimate the upper J_{sc} limit given by our front- and back-junction geometries. Since recombination is absent, the current density generated by absorbed light in silicon equals the external quantum efficiency $EQE(\lambda)$. We calculate the internal quantum efficiency IQE(λ) using the following equation:

$$IQE(\lambda) = \frac{EQE(\lambda)}{1 - R(\lambda)} \quad (4)$$

where $R(\lambda)$ is the simulated spectral reflection. Fig. 4(b) shows the calculated internal quantum efficiency (IQE) and the reflectance for the front- and back-junction organic-silicon solar cells. For both geometries we obtain a reflection minimum within the wavelength range from 500 to 650 nm.

Fig. 5 shows two pie diagrams of the short-circuit current density (J_{sc}) generated through absorption in silicon and J_{sc} losses caused by reflection and parasitic absorption within the PEDOT:PSS layer for the (a) a front-junction and (b) back-junction organic-silicon solar cell.

Please cite this article as: D. Zielke, et al., Organic-silicon heterojunction solar cells on n-type silicon wafers: The BackPEDOT concept, Solar Energy Materials and Solar Cells (2014), http://dx.doi.org/10.1016/j.solmat.2014.05.022

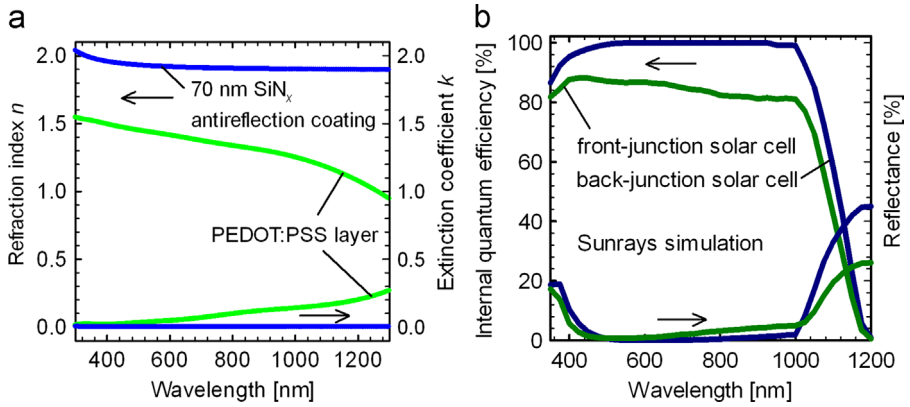

Fig. 4. (a) Measured spectrally resolved $n(\lambda)$ and $k(\lambda)$ values of a 100 nm thick PEDOT:PSS (Clevious F HC Solar) layer and of a SiN_x antireflection coating. (b) Simulated internal quantum efficiency and reflectance for front-junction (green line) and back-junction (blue line) organic-silicon solar cells. (For interpretation of the references to color in this figure legend, the reader is referred to the web version of this article.)

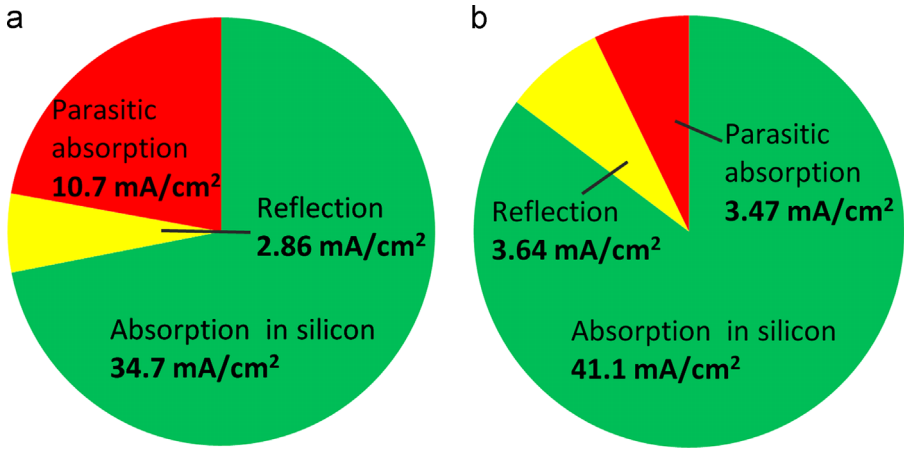

Fig. 5. Pie diagrams of the short-circuit current density (J_{sc}) generated through absorption in silicon and J_{sc} losses caused by reflection and parasitic absorption in the PEDOT:PSS for the (a) front-junction and (b) BackPEDOT solar cell.

For the back-junction geometry we observe a current-density loss of 3.6 mA/cm^2 due to reflection. For the front-junction geometry J_{sc} loss of 2.9 mA/cm^2 is reduced due to the lower refractive index of the PEDOT:PSS front layer compared to a standard SiN_x antireflection coating, as shown in Fig. 4(a). The parasitic light absorption of the BackPEDOT cell results in a total J_{sc} loss of 3.5 mA/cm^2. For the front-junction organic-silicon cell we observed a total J_{sc} loss of 10.7 mA/cm^2, largely caused by the absorption within the PEDOT:PSS layer caused by the higher extinction coefficient compared to a SiN_x antireflection coating, as shown in Fig. 4(a). This relatively large J_{sc} loss limits the maximum J_{sc} in the front-junction device to only 34.7 mA/cm^2. For the BackPEDOT solar cell, on the other hand, a realistic maximum, J_{sc} of 41.1 mA/cm^2 is reachable. Combining this J_{sc} value with the realistically reachable V_{oc} of 668 mV (see Section 4) and assuming an upper fill-factor FF=83%, the BackPEDOT cell has an efficiency potential of 22.8 %.

6. Solar cells

6.1. Experimental details

6.1.1. Front-junction solar cell

Fig. 2(a) shows the front-junction organic-silicon solar cell structure. In the cell process, we started with a 300 μm thick phosphorus-doped (100)-oriented float-zone (FZ) n-type silicon wafer with a resistivity of 1.5 Ω cm. After RCA-cleaning, the front surface was protected with a 100 nm thick SiN_x layer. Subsequently after RCA-cleaning, a BSF was formed by phosphorus diffusion from a $POCl_3$ source in a quartz-tube furnace at a temperature of 850 °C. The resulting n^+ BSF had a sheet resistance of 152 ± 9 Ω/sq. Next, the front SiN_x protecting layer and the phosphorus silicate glass were removed in diluted hydrofluoric acid (HF) and the wafer rear side was protected by a SiN_x protection layer. After RCA cleaning, the front surface was RP-textured in a KOH/iso-propanol solution and SiN_x was removed in a diluted HF solution. Subsequently, aluminum was deposited on the entire rear surface by electron beam evaporation. After rear side metallization, the samples were stored in air for approximately 30 h to grow a native tunneling oxide on the front side. Subsequently, a PEDOT:PSS (Clevios F HC Solar) layer was deposited by spin-coating on the entire front surface at 1000 revolutions per minute (rpm) for 10 s and subsequently 2000 rpm for 30 s, which results in a thickness of 100 nm. The thickness was measured on a planar glass reference sample by scratching a trench into the PEDOT:PSS layer. The depth of the trench was measured using a profilometer (Dektak 150, Veeco). Finally, a Ti/Pd/Ag grid was evaporated onto the PEDOT:PSS through a shadow mask by electron beam evaporation.

6.1.2. BackPEDOT solar cell

Fig. 2(b) shows the BackPEDOT cell. In our process, we started with an n-type Czochralski (Cz) phosphorus-doped silicon wafer with a resistivity of 4–5 Ω cm and a thickness of 160 μm.

Please cite this article as: D. Zielke, et al., Organic-silicon heterojunction solar cells on n-type silicon wafers: The BackPEDOT concept, Solar Energy Materials and Solar Cells (2014), http://dx.doi.org/10.1016/j.solmat.2014.05.022

Table 1
Parameters of the best front-junction and back-junction organic-silicon solar cells measured at 100 mW/cm^2 ('one sun') at a temperature of 25 °C. The aperture area of the n-type organic-silicon solar cells is 4 cm^2.

Organic-silicon solar cell	V_{oc} (mV)	J_{sc} (mA cm^{-2})	FF (%)	*pFF* (%)	η(%)	pη(%)	R_s (Ω cm^{-2})
Front-junction	603	29.0	70.6	72.8	12.3	12.7	0.92
Front-junction	601	29.2	69.6	72.6	12.2	12.7	0.99
Back-junction	653	39.7	67.2	82.0	17.4	21.2	2.88
Back-junction	663	39.0	66.3	81.3	17.1	21.0	3.35

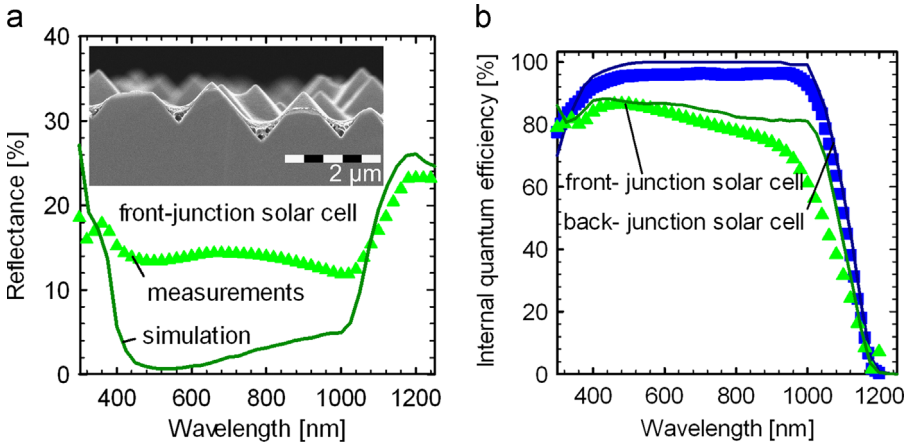

Fig. 6. (a) Measured and simulated reflectance of our front-junction organic-silicon solar cell. The inset shows a scanning electron microscopy image of our PEDOT:PSS layer covering a random-pyramid-textures silicon surface. (b) Measured (symbols) and simulated (lines) internal quantum efficiencies of a front-junction organic-silicon cell (green line/symbols) and a BackPEDOT (blue line/symbols). (For interpretation of the references to color in this figure legend, the reader is referred to the web version of this article.)

After RCA-cleaning, the wafer was protected on both surfaces with a 100 nm thick SiN_x layer. On the front surface, a 2×2 cm^2 diffusion window was opened by laser ablation (frequency-doubled Nd:YVO_4 laser, SuperRapid, Lumera Laser). Within the ablated window the silicon surface was RP-textured in a KOH/iso-propanol solution. Subsequently after RCA-cleaning, a phosphorus diffusion was performed from a $POCl_3$ source in a quartz-tube furnace at 850 °C forming a front surface field (FSF) with a sheet resistance of 114 ± 11 Ω/sq. After removing the protecting SiN_x layer and the phosphorus silicate glass in diluted hydrofluoric acid, an 0.24 nm AlO_x tunneling layer was atomic-layer-deposited (FlexAL, Oxford Instruments) on the front surface. Next, a 20 µm thick aluminum grid with a finger spacing of 1 mm was deposited through a nickel shadow mask by electron beam evaporation. After metallization, the front surface was covered by a 10 nm surface-passivating SiN_x layer with a refractive index of 2.4 and by a 70 nm SiN_x antireflection layer with a refractive index of 1.9 on top. Both SiN_x layers were deposited at a temperature of 330 °C using PECVD. Afterwards, the samples were stored in air for 24 h to form a native oxide at the rear surface. Next, a PEDOT:PSS layer with a thickness of 140 ± 7 nm (Clevios F HC Solar) was deposited by spin-coating on the entire rear at 500 revolutions per minute (rpm) for 10 s and subsequently 1000 rpm for 30 s. The sample was then dried on a hotplate in air at 130 °C for 30 s. Finally, the entire rear surface was metalized by electron beam evaporated silver.

6.2. Solar cell results

Illuminated current–voltage (*I–V*) characteristics at an illumination intensity of 100 mW/cm^2 ('one sun'), external quantum efficiency (EQE), and reflectance are measured using a commercial measurement system (LOANA System, pv-tools, Hamelin, Germany) with an aperture area mask of 2×2 cm². We correct the spectral mismatch by comparing the EQE of our solar cell with an EQE reference solar cell measured under standard testing conditions at Fraunhofer ISE CalLab.

Table 1 summarizes measured solar cell parameters of our front-junction and back-junction organic-silicon solar cells. The best front-junction solar cell shows V_{oc} of 603 mV and J_{sc} of 29.2 mA/cm^2. Note that despite the moderate series resistance of $R_s=0.92$ Ω cm^2 we obtain a relatively low fill factor *FF* of only 70.6 % and a poor pseudo *FF* of only 72.8 %. The achieved solar cell efficiency of 12.3% is amongst the highest front-junction organic-silicon solar cell efficiencies reported so far.

In order to fully exploit the potential of combining organic photovoltaics with silicon-based photovoltaics, we have applied the organic PEDOT:PSS layer to the planar rear of a c-Si wafer and implemented an n^+ FSF plus an effective dielectric passivation. With this novel BackPEDOT solar cell concept, we achieve a remarkably high open-circuit voltage V_{oc} of 663 mV and a very high short-circuit current density J_{sc} of 39.7 mA/cm^2. Despite the relative low fill factor *FF* of up to 67.2 %, we achieve energy conversion efficiencies of up to 17.4%. By introducing the Back-PEDOT concept, we improved the efficiency of organic-silicon solar cells by 5% absolute compared to the best results reported so far for front-junction organic-silicon solar cells.

Implementing PEDOT:PSS to the rear surface and passivating the n^+ front surface field with SiN_x leads to a V_{oc} improvement in the range of 50 to 62 mV. This improvement correlates well with our J_0 measurements, where V_{oc} improvement of 54 mV was calculated. J_{sc} improvement in the range of 9.8 to 10.7 mA/cm^2, on the other hand, is larger than our simulated improvement of 6.4 mA/cm^2. There are two reasons for this discrepancy. First, the light reflection from the front-junction solar cell is larger compared to the simulation. Fig. 6(a) shows the measured and simulated reflection. The inset of Fig. 6(a) shows a scanning electron microscopy image of our PEDOT:PSS layer covering a random-pyramid-textured silicon surface. It is obvious that the PEDOT:PSS layer flattens the surface morphology and therefore

Please cite this article as: D. Zielke, et al., Organic-silicon heterojunction solar cells on *n*-type silicon wafers: The BackPEDOT concept, Solar Energy Materials and Solar Cells (2014), http://dx.doi.org/10.1016/j.solmat.2014.05.022

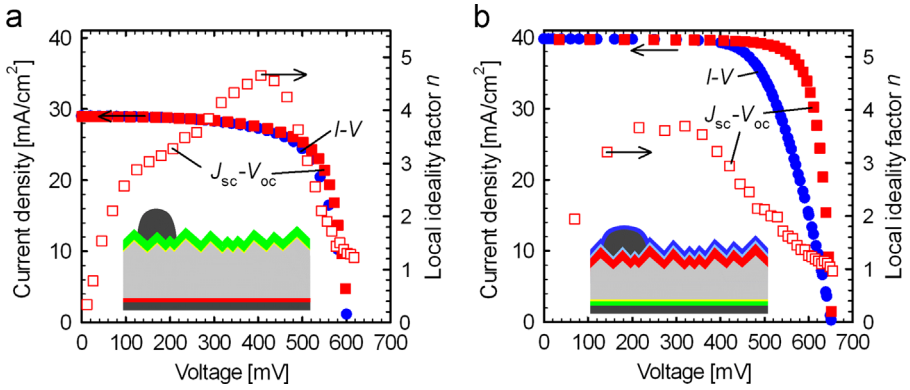

Fig. 7. Illuminated current density–voltage (J–V), short-circuit current density - open-circuit voltage ($J_{sc}-V_{oc}$) measurements and the local ideality factor n of the J_{sc}–V_{oc} curve for a (a) front-junction organic-silicon heterojunction and (b) a BackPEDOT solar cell.

increases the reflection. The difference between the measured and the simulated reflectance leads to J_{sc} loss of 4.25 mA/cm^2 for the front-junction solar cell. The second reason for the observed discrepancy is the increased recombination of the surfaces of our front-junction organic-silicon solar cell. Fig. 6(b) shows the measured and simulated IQE curves. We observe a clear deviation between the simulated and measured IQE at higher wavelengths for the front-junction organic-silicon solar cell. Since high-purity float-zone silicon is used, this deviation can only be caused by an increased rear surface recombination. We are not surprised about high recombination at the rear surface since n^+-BSF is not passivated and fully metalized. Increased recombination at the rear surface of our front-junction solar cell leads to a decreasing IQE curve for wavelengths larger than 600 nm. The difference between the measured and simulated IQE leads to J_{sc} loss of 2.78 mA/cm^2 compared to a J_{sc} loss of only 1.84 mA/cm^2 for our back-junction solar cell.

Fig. 7 shows illuminated current–voltage (J–V), J_{sc}–V_{oc} and measurements of the local ideality factor n of the J_{sc}–V_{oc} curve for our best (a) front-junction and (b) BackPEDOT solar cells, respectively. The ideality factor is the inverse slope of the semi-logarithmic J_{sc}–V_{oc} curve. Values larger than unity are caused by low shunt-resistances and by injection-dependent recombination in the bulk or/and at the surfaces. The influence of the series resistance on the n value can be avoided by analyzing the J_{sc}–V_{oc} curve.

The highest n values of the front-junction solar cell are observed at lower voltages than the highest n values of the back-junction solar cell. We attribute this finding to the injection-dependent recombination at the entirely metalized n^+ BSF. For the front-junction solar cell, the ideality factor increases to $n(pV_{mpp})=3$ at the pseudo maximum power-point voltage $pV_{mpp}=512$ mV limiting the pseudo fill-factor pFF to a value of only 72.8 %. For the BackPEDOT solar cell – where front and rear surfaces are passivated – we obtain a relatively low n ($pV_{mpp}=565$ mV)$=1.5$ allowing pFF values of 82.0 %. By comparing J_{sc}–V_{oc} and J–V curves of our back-junction organic-silicon solar cell one can clearly notice a shift of the J–V curve towards lower voltages caused by the series resistance. Measurements of the series resistance (R_s) at the maximum power-point of the J–V curve using the double-light method reveal a strong scattering in R_s values between 2.88 and 3.35 Ω cm^2. The reason why R_s of the back-junction solar cells is increased compared to the front-junction solar cells is not fully understood yet. One suggestion is the state of our PEDOT:PSS chemical. We used the same PEDOT:PSS solution for the front and the back-junction, however, we fabricated the back-junction solar cells several months after the front-junction cells. The PEDOT:PSS solution might have degraded during this period. More detailed investigations are necessary to understand the current transport mechanism through the organic-silicon junction to reduce series resistance losses. For the lowest R_s value of 2.88 Ω cm^2 we measure a FF of 67.2 % and an energy conversion efficiency of 17.4%, which is the highest reported value for organic-silicon heterojunction solar cells so far. Analyzing the J_{sc}–V_{oc} curve and, hence, neglecting the influence of the series resistance, we measure a pseudo fill factor of $pFF=82.0$ % and a pseudo efficiency of $p\eta=21.2$% for our best BackPEDOT cell.

7. Conclusions

We have introduced a novel solar cell concept, the so-called BackPEDOT solar cell, based on a back-junction PEDOT:PSS-silicon heterojunction. Electrical and optical measurements in combination with ray-tracing simulations have shown that the BackPEDOT cell could realistically reach J_{sc} of 41.1 mA/cm², V_{oc} of 668 mV and an efficiency of 22.8 %. We have also fabricated first BackPEDOT experimental devices, which achieved a remarkably high V_{oc} of 663 mV and J_{sc} of 39.7 mA/cm^2. The IV curves showed a good ideality, as reflected by pseudo fill-factor of up to 82.0 %. However, the actual fill-factors were largely limited by a high series resistance which was in the range between 2.88 and 3.35 Ω cm^2. Despite the relative low FF of 67.2 %, we have achieved an energy conversion efficiency of 17.4%, which is by far the highest energy conversion efficiency obtained for any organic-silicon solar cell to date. Note that our 17.4% efficient record solar cell is fully limited by series resistance losses and neglecting the influence of the series resistance, we have extracted a pseudo efficiency of 21.2% for our best BackPEDOT cell.

References

[1] P.J. Cousins, D.D. Smith, H.C. Luan, J. Manning, T.D. Dennis, A. Waldhauer, K.E. Wilson, G. Harley, G.P. Mulligan. Gen III: Improved performance at lower cost, in: Proceedings of the 35th IEEE Photovoltaic Specialists Conference, Honolulu, USA, 2010, pp. 275–278.

[2] T. Kinoshita, D. Fujishima, A. Yano, A. Ogane, S. Tohoda, K. Matsuyama, Y. Nakamura, N. Tokuoka,H. Kanno, H. Sakata, M. Taguchi and E. Maruyama, The approaches for high efficiency HIT^{TM} solar cell with very thin (< 100 μm) silicon wafer over 23%, In: Proceedings of the 26th European Photovoltaic Solar Energy Conference, Hamburg, Germany, 2011, pp. 871–874.

[3] N. Mingirulli, J. Haschke, R. Gogolin, R. Ferré, T. Schulze, J. Düsterhoft, N.-P. Harder, L. Korte, R. Brendel, B. Rech, Efficient interdigitated back-contacted silicon heterojunction solar cells, Phys. Status Solidi RRL 5 (2011) 159–161.

[4] M. Bivour, C. Meinhard, D. Pysch, C. Reichel, K.U. Ritzau, A. Hermle, S.W. Glunz, n-Type silicon solar cells with amorphous/scystalline silicon heterojunction rear emitter, in: Proceedings of the 35th IEEE Photovoltaic Specialists Conference, Honolulu, USA, 2010, pp. 1304 – 1308.

[5] L. He, C. Jiang, H. Wang, D. Lai, Rusli, High efficiency planar Si/organic heterojunction hybrid solar cells, Appl. Phys. Lett. 100 (2012) 073503.

[6] I. Khatri, Z. Tang, Q. Liu, R. Ishikawa, K. Ueno, H. Shirai, Green-tea modified multiwalled carbon nanotubes for efficient poly(3,4-ethylenedioxythiophene):

Please cite this article as: D. Zielke, et al., Organic-silicon heterojunction solar cells on n-type silicon wafers: The BackPEDOT concept, Solar Energy Materials and Solar Cells (2014), http://dx.doi.org/10.1016/j.solmat.2014.05.022

poly(stylenesulfonate)/n-silicon hybrid solar cell, Appl. Phys. Lett. 102 (2013) 063508.

[7] Z. Tang, Q. Liu, I. Khatri, R. Ishikawa, K. Ueno, H. Shirai, Optical properties and carrier transport in c-Si/conductive PEDOT:PSS(GO) composite heterojunctions, Phys. Status Solidi C 9 (2012) 2075–2078.

[8] J.-Y. Chen, M.-H. Yu, S.-F. Chang, K.W. Sun, Highly efficient poly(3,4- thylenedioxythiophene):poly(styrenesulfonate)/Si hybrid solar cells with imprinted nanopyramid structures, Appl. Phys. Lett 103 (2013) 133901.

[9] K.A. Nagamatsu, S. Avasthi, J. Jhaveri, J.C. Sturm, A 12% Efficient Silicon/PEDOT:PSS Heterojunction Solar Cell Fabricated at < 100 C, IEEE J. Photovolt. 4 (2014) 260–264.

[10] J. Schmidt, V. Titova, D. Zielke, Organic-silicon heterojunction solar cells: open-circuit voltage potential and stability, Appl. Phys. Lett. 103 (2013) 183901.

[11] T. Lauinger, J. Schmidt, A.G. Aberle, R. Hezel, Record low surface recombination velocities on 1 Ω cm p-silicon using remote plasma silicon nitride passivation, Appl. Phys. Lett. 68 (1996) 1233.

[12] D. Zielke, J.H. Petermann, F. Werner, B. Veith, R. Brendel, J. Schmidt, Contact passivation in silicon solar cells using atomic-layer-deposited aluminum oxide layers, Phys. Status Solidi RRL 5 (2011) 298–300.

[13] R.A. Sinton, A. Cuevas, Contactless determination of current–voltage characteristics and minority-carrier lifetimes in semiconductors from quasi-steady-state photoconductance data, Appl. Phys. Lett. 69 (1996) 2510.

[14] J. Bullock, D. Yan, A. Cuevas, Passivation of aluminium–n+ silicon contacts for solar cells by ultrathin Al2O3 and SiO2 dielectric layers, Phys. Status Solidi RRL 7 (2013) 946–949.

[15] R. Brendel, Sunrays 1.3, MPI-FKF D-70569 Stuttgart, Germany.

Please cite this article as: D. Zielke, et al., Organic-silicon heterojunction solar cells on *n*-type silicon wafers: The BackPEDOT concept, Solar Energy Materials and Solar Cells (2014), http://dx.doi.org/10.1016/j.solmat.2014.05.022